Inorg. Chem. **2006**, *45*, 4461–4467

Testing Bridge-Mediated Differences in Dinuclear Valence Tautomeric Behavior

Sofi Bin-Salamon,[†] Scott H. Brewer,[†] Ezra C. Depperman,[‡] Stefan Franzen,[†] Jeff W. Kampf,[§] Martin L. Kirk,*[,‡] R. Krishna Kumar,[†] Simon Lappi,[†] Katrina Peariso,[‡] Kathryn E. Preuss,*[,†] and David A. Shultz*[,†]

Department of Chemistry, North Carolina State University, Raleigh, North Carolina 27695-8204, Department of Chemistry, University of New Mexico, Albuquerque, New Mexico 87131, and Department of Chemistry, University of Michigan, Ann Arbor, Michigan 48109-1055

Received January 30, 2006

Two structurally characterized dinuclear valence tautomers are described. Cobalt ions are bridged by *p*- and *m*-phenylene units connected to 2,2′-bipyridines. X-ray crystal structures show that the molecules are in the [(Co^{III})-(Co^{III})] forms at ca. 125 K, while spectroscopic studies show that both molecules can achieve the [(Co^{II})(Co^{II})] form above 400 K and confirm the [(Co^{III})(Co^{III})] form below 10 K. Magnetic susceptibility studies are also included. Our results highlight the necessity of studying both crystalline and amorphous samples to distinguish the effects of intrinsic electronic structure and intermolecular forces on valence tautomeric behavior.

Introduction

Valence tautomerism (VT) is defined as a reversible intramolecular metal−ligand electron transfer that may be coupled to a spin-crossover at the metal center.[1−4] To date, most VT complexes have been prepared from redox-active transition metals, such as Co or Mn, and dioxolene-type ligands in which the dianion oxidation state (catecholate, Cat) and radical anion oxidation state (semiquinone, SQ) are both accessible, with diimine-type ancillary ligands (N−N) to complete the coordination sphere.[5−9] In the case that Co is the redox-active metal, the reduced Co^{II} ion possesses the electronic configuration $(d_{xy,xz,yz})^5(d_{x^2-y^2},d_{z^2}*)^2$ and is high-spin (hs), while the oxidized Co^{III} ion possesses a $(d_{xy,xz,yz})^6$-$(d_{x^2-y^2},d_{z^2}*)^0$ electronic configuration and is low-spin (ls). Since dioxolene ligand orbitals lie close in energy to the metal d-orbitals, giving rise to a high degree of metal−ligand covalency, occupation of the $d_{x^2-y^2}$ and d_{z^2} σ* orbitals in the hs-Co^{II} form results in longer Co−dioxolene bond lengths. The longer, weaker bonds in the hs-Co^{II} form of the valence tautomer are characterized by a higher density of vibrational levels compared to those in the ls-Co^{III} form and consequently result in an increase in the entropic contribution to the Gibbs free energy in the hs-Co^{II} state. Since it is the large $\Delta S°$ that results in a change in the sign of $\Delta G°$ as a function of temperature, valence tautomeric equilibria (and spin-crossover equilibria) are said to be "entropy driven" phenomena.

$$\text{hs-Co}^{\text{II}}(\text{SQ})_2(\text{N}-\text{N}) \overset{K_{\text{VT}}}{\rightleftharpoons} \text{ls-Co}^{\text{III}}(\text{SQ})(\text{Cat})(\text{N}-\text{N})$$

Several reports suggest that *inter*molecular interactions and solvation make a major contribution to $\Delta S°$.[1,10−12] In the crystalline state, intermolecular interactions can give rise to molecular bistability,[13,14] and VT complexes are therefore potential candidates for molecular devices and sensors.

* To whom correspondence should be addressed. E-mail: mkirk@unm.edu (M.L.K.), kpreuss@uoguelph.ca (K.E.P.), David_Shultz@ncsu.edu (D.A.S.).
[†] North Carolina State University.
[‡] University of New Mexico.
[§] University of Michigan.

(1) Shultz, D. A. Valence Tautomerism in Dioxolene Complexes of Cobalt. In *Magnetism: Molecules to Materials II: Molecule-based Materials;* Miller, J. S., Drillon, M., Eds.; Wiley-VCH: New York, 2001; pp 281−306.
(2) Pierpont, C. G. *Coord. Chem. Rev.* **2001**, *216*, 99.
(3) Helton, M. E.; Gebhart, N. L.; Davies, E. S.; McMaster, J.; Garner, C. D.; Kirk, M. L. *J. Am. Chem. Soc.* **2001**, *123*, 10389.
(4) Ratera, I.; Ruiz-Molina, D.; Renz, F.; Ensling, J.; Wurst, K.; Rovira, C.; Gütlich, P.; Veciana, J. *J. Am. Chem. Soc.* **2003**, *125*, 1462.
(5) Gütlich, P.; Dei, A. *Angew. Chem., Int. Ed. Engl.* **1997**, *36*, 2734.
(6) Shimazaki, Y.; Tani, F.; Fukui, K.; Naruta, Y.; Yamauchi, O. *J. Am. Chem. Soc.* **2003**, *125*, 10512.
(7) Rall, J.; Wanner, M.; Albrecht, M.; Hornung, F. M.; Kaim, W. *Chem.—Eur. J.* **1999**, *5*, 2802.
(8) Lange, W.; Werner, T. *Chem. Ber.* **1989**, *122*, 1765.
(9) Jung, O.-S.; Lee, Y.-A.; Pierpont, C. G. *Synth. Met.* **1995**, *71*, 2019.
(10) Bubnov, M. P.; Cherkasov, V. K.; Abakumov, G. A. *Metall. Khim.* **1993**, *6*, 63. Abakumov, G. A.; Cherkasov, V. K.; Bubnov, M. P.; Ellert, O. G.; Dobrokhotova, Zh. V.; Zakharov, L. N.; Struchkov, Y. T. *Dokl. Ross. Akda. S-kh. Nauk* **1993**, *328*, 332.
(11) LaBute, M. X.; Kulkarni, R. V.; Endres, R. G.; Cox, D. L. *J. Chem. Phys.* **2002**, *116*, 3681.
(12) Cador, O.; Dei, A.; Sangregorio, C. *Chem. Commun.* **2004**, 652.

10.1021/ic060170y CCC: $33.50
Published on Web 04/26/2006

Chart 1

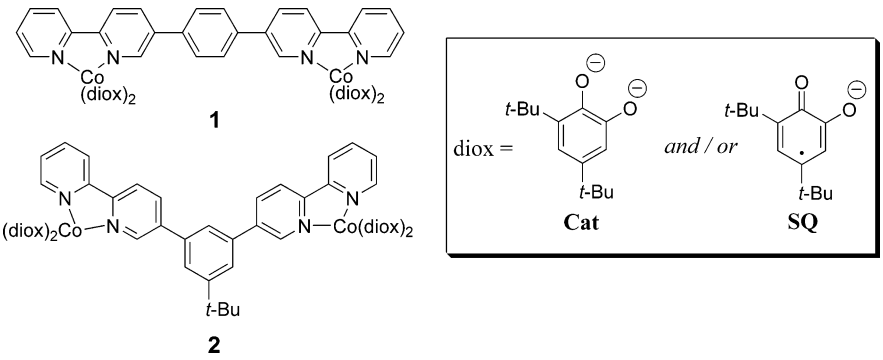

In principle, dinuclear valence tautomers may possess three metastable states: $(Co^{III})_2$, $[(Co^{II})(Co^{III})]$, and $(Co^{II})_2$. As such, they form the basis for ternary information storage at the molecular level.[15] Extending this reasoning, higher order molecular logic devices could be prepared by coupling more than two valence tautomeric units. However, to adopt this building-block model, one must design molecules that (a) possess multiple metastable states that are accessible over a desirable temperature range and (b) possess the proper degree of communication between VT units such that each state may be discretely addressable. In an attempt to meet these requirements, several dinuclear VT complexes designed using a modified dioxolene as the bridging ligand between two cobalt centers have been reported.[15−18] Dei and co-workers[17] recently published a tetraoxolene-based dinuclear VT and demonstrated from electron paramagnetic resonance (EPR) and magnetic susceptibility experiments that the complex exhibits strong intramolecular electronic coupling between the magnetic centers because of the interconversion between the $S = {}^1/_2$ and $S = {}^3/_2$ states. The interconversion between the two states corresponds to the population of the $(Co^{III})_2$ at low temperature and the intermediate $[(Co^{II})(Co^{III})]$ electronic state at high temperature. Interestingly, the $(Co^{II})_2$ state is not observed within a reasonable temperature range for either solution or solid-state experiments. This may be because further oxidation of the tetraoxolene would require removal of an electron from a low-lying orbital, which would in turn increase the enthalpy difference between the $[(Co^{II})(Co^{III})]$ and the $(Co^{II})_2$ forms. Another drawback of the tetraoxolene design is that it does not lend itself as a building block for coupling of more than two VT centers. Where previous attempts to create dinuclear valence tautomers utilize modifications of the dioxolene ligand, our present effort centers on a dinuclear design through modification of the diimine (bipyridine) ligand. We hypothesize that bipyridine has the potential to serve as an electronic coupling unit given that back-bonding between the cobalt center and bipyridine affords some degree of electronic delocalization onto the bipyridine molecule (see Chart 1).[19] It should be noted that Jung and co-workers have prepared a dinuclear VT complex using 2,2′-bipyrimidine as the bridging ancillary ligand; however, there was no reported evidence of valence tautomeric switching of both cobalt centers.[20] Herein, we report the first two structurally, magnetically, and spectroscopically characterized dinuclear VT complexes (**1** and **2**) wherein the bridging ligand is the ancillary diimine and all three possible valence tautomeric forms ($(Co^{III})_2$, $[(Co^{II})(Co^{III})]$, and $(Co^{II})_2$) exist below 500 K. We use a combination of magnetic susceptibility, electronic absorption spectroscopy, and X-ray absorption spectroscopy (XAS) at the Co K-edge to probe the effects of environment on VT equilibria.

Results

Synthesis. The complexes **1** and **2** were synthesized as shown in Scheme 1. The reaction of 5-bromo-2,2′-bipyridine **3** [21] with bis(boronic ester) **4** [22] gives the bis(bipyridine) ligand **5**. Compound **5** is known,[23] but we preferred to prepare it using Suzuki coupling methodology common in our laboratory. Likewise, bromide **3** was reacted with bis(boronic ester) **6** [22] yielding the previously unknown ligand **7**. The bis(bipyridine) ligands **5** and **7** were reacted with Co_4(3,5-di-*tert*-butylorthosemiquinone)$_8$ **9**,[24] according to standard literature procedure,[25] generating dinuclear VT complexes **1** and **2**.

Crystallography. X-ray quality single crystals of **1** and **2** were grown by slow evaporation of methylene chloride/toluene solutions. As a result, toluene was incorporated into the crystal structures in a ratio of 2:1 in the case of complex **1** and a ratio of 3:1 in the case of complex **2**. In both complexes, the Co−O bond lengths and the dioxolene C−O and C−C bond lengths are consistent with the $(Co^{III})_2$

(13) Adams, D. M.; Dei, A.; Rheingold, A. L.; Hendrickson, D. N. *J. Am. Chem. Soc.* **1993**, *115*, 8221.
(14) Jung, O.-S.; Jo, D. H.; Lee, Y.-A.; Conklin, B. J.; Pierpont, C. G. *Inorg. Chem.* **1997**, *36*, 19.
(15) Bodner, S. H.; Caneschi, A.; Dei, A.; Shultz, D. A.; Sorace, L. *Chem. Commun.* **2001**, 2150.
(16) Dei, A.; Gatteschi, D.; Sangregorio, C.; Sorace, L. *Acc. Chem. Res.* **2004**, *37*, 827.
(17) Carbonera, C.; Dei, A.; Letard, J.-F.; Sangregorio, C.; Sorace, L. *Angew. Chem., Int. Ed.* **2004**, *43*, 3136.
(18) Tao, J.; Maruyama, H.; Sato, O. *J. Am. Chem. Soc.* **2006**, 128 (6), 1790−1791.
(19) Adams, D. A.; Noodleman, L.; Hendrickson, D. N. *Inorg. Chem.* **1997**, *36*, 3966.
(20) Jung, O.-S.; Jo, D. H.; Lee, Y.-A.; Chae, H. K.; Sohn, Y. S. *Bull. Chem. Soc. Jpn.* **1996**, *69*, 2211.
(21) Schwab, P. F. H.; Fleischer, F.; Michl, J. *J. Org. Chem.* **2002**, *67*, 443.
(22) Shultz, D. A.; Lee, H. L.; Kumar, R. K.; Gwaltney, K. *J. Org. Chem.* **1999**, *64*, 9124.
(23) Baxter, P. N. W. *J. Org. Chem.* **2000**, *65*, 1257.
(24) Buchanan, R. M.; Fitzgerald, B. J.; Pierpont, C. G. *Inorg. Chem.* **1979**, *18*, 3439.
(25) Buchanan, R. M.; Pierpont, C. G. *J. Am. Chem. Soc.* **1980**, *102*, 4951.

Scheme 1. Synthetic Outline for Dinuclear Valence Tautomers **1** and **2**

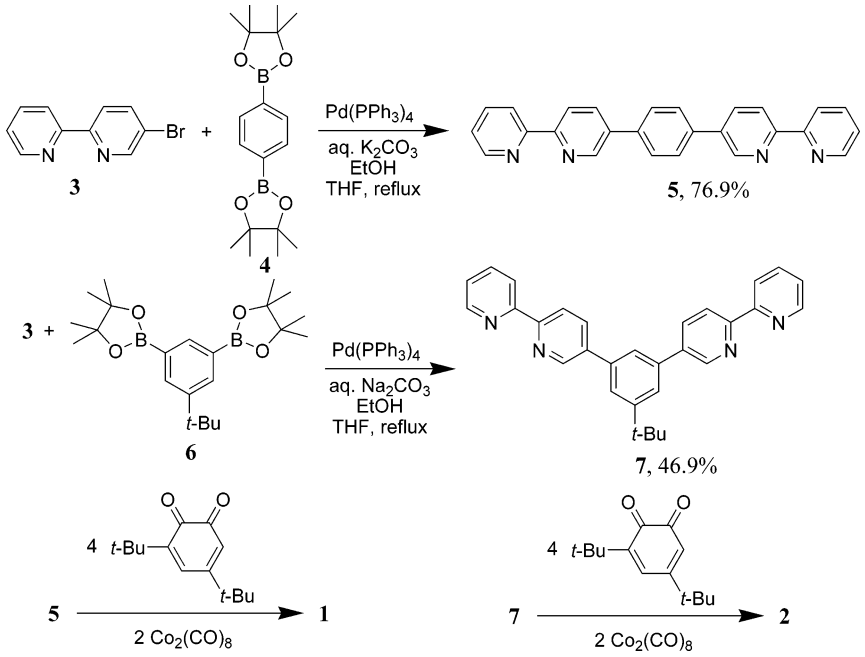

formulation (i.e., one SQ and one Cat at each Co center) in the ca. 125 K structure. In neither complex **1** nor **2** is the central phenyl ring strictly coplanar with the bipyridine rings, implying some flexibility in the ligand "backbone" such that rotation around σ bonds may be expected. Nevertheless, for both complexes, the crystal structure shows only the isomer wherein both Co centers are on the same side of the molecule. ORTEP diagrams of complex **1** and **2** are shown in Figures 1 and 2, respectively. Crystal packing gives rise to short intermolecular distances, which are highlighted for both complexes in Figure 3. Some important bond lengths, torsion angles, and intermolecular contacts are given in Table 1. Further crystal data can be found in the Supporting Information.

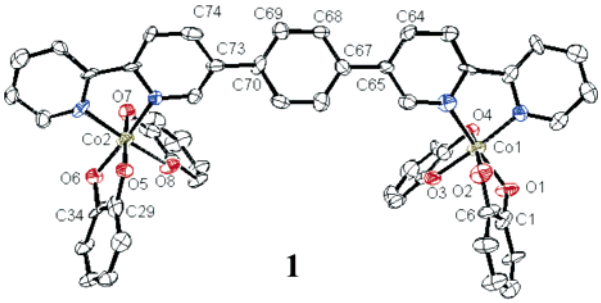

Figure 1. Thermal ellipsoid plot for **1**; monoclinic $P2_1/c$; $a = 16.862(3)$, $b = 26.337(5)$, $c = 26.737(5)$ Å; $\beta = 124.136(3)°$. The data were collected at $T = 123$ K. Hydrogen atoms, dioxolene *tert*-butyl groups, and toluene molecules were omitted for clarity.

Variable-Temperature Magnetic Susceptibility Studies. Magnetic data for toluene-free microcrystalline samples of **1** and **2** were collected on a SQUID magnetometer in an applied DC field of 1 T. The data are shown in Figure 4 as plots of $\chi_{para}T$ vs T. The magnetic data for **2** show $\chi_{para}T$ approximately equal to 4.1 (emu·K)/mol at 400 K and decreasing with decreasing temperature. The data begin to plateau at 50 K with a $\chi_{para}T$ value of ~2.2 (emu·K)/mol

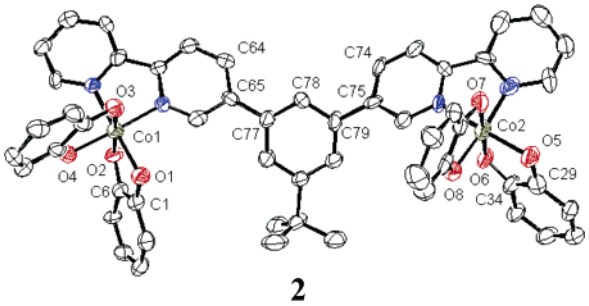

Figure 2. Thermal ellipsoid plot for **2**; monoclinic $P2_1/n$; $a = 20.633(4)$, $b = 19.207(3)$, $c = 24.055(4)$ Å; $\beta = 95.452(7)°$. The data were collected at $T = 133$ K. Hydrogen atoms, dioxolene *tert*-butyl groups, and toluene molecules were omitted for clarity.

before intermolecular exchange interactions start to dominate and reduce the effective moment of the sample at lower temperatures. In contrast, the magnetic data for **1** show a considerably lower $\chi_{para}T$ value at 400 K (~2.8 (emu·K)/mol). The data for **1** begin to plateau at 50 K with a $\chi_{para}T$ value of ~0.75 (emu·K)/mol. Intermolecular exchange interactions dominate the magnetic data at temperatures below ~10 K, resulting in a sharp drop in the $\chi_{para}T$ values. For a dinuclear VT in the $(Co^{II})_2$ form, the estimated maximum value of $\chi_{para}T$ is ca. 5 (emu·K)/mol (i.e., two uncorrelated $Co^{II}(SQ)_2$ moieties), whereas for the mixed-valent $[(Co^{II})(Co^{III})]$ form, the estimated maximum value of $\chi_{para}T$ is ca. 2.9 (emu·K)/mol (i.e., uncorrelated $Co^{II}(SQ)_2$ and $Co^{III}(SQ)(Cat)$ moieties). Finally, the isovalent $(Co^{III})_2$ form should exhibit $\chi_{para}T$ equal to 0.75 (emu·K)/mol because of the two uncorrelated SQ $S = {}^1/_2$ spins. Given these estimates, it appears that in the case of **2** we are observing tautomerism between the $(Co^{II})_2$ form and the $[(Co^{II})(Co^{III})]$ form in the 400 to 50 K temperature range, whereas compound **1** shows tautomerism between the $[(Co^{II})(Co^{III})]$ form and the $(Co^{III})_2$ form in the same temperature range. It should be noted that, for both **1** and **2**, $\chi_{para}T$ continues to

Table 1. Important Distances (Å) and Angles (deg) for **1** and **2** As Determined by Single-Crystal X-ray Diffraction

$C_{82}H_{98}N_4O_8Co_2$ (**1**·2C_7H_8)				$C_{107}H_{130}N_4O_8Co_2$ (**2**·3C_7H_8)			
Metal Bond Lengths (Å)							
Co1−O1	1.893(6)	Co2−O5	1.870(6)	Co1−O1	1.893(6)	Co2−O5	1.883(6)
Co1−O2	1.930(6)	Co2−O6	1.871(6)	Co1−O2	1.914(6)	Co2−O6	1.899(6)
Co1−O3	1.843(6)	Co2−O7	1.901(6)	Co1−O3	1.865(6)	Co2−O7	1.860(6)
Co1−O4	1.872(6)	Co2−O8	1.900(6)	Co1−O4	1.861(6)	Co2−O8	1.874(6)
Co1−N1	1.924(8)	Co2−N3	1.938(8)	Co1−N1	1.930(7)	Co2−N3	1.917(9)
Co1−N2	1.942(8)	Co3−N4	1.938(8)	Co1−N2	1.922(7)	Co3−N4	1.894(7)
Semiquinone Rings (Å)							
C1−O1	1.307(11)	C43−O7	1.329(12)	C1− O1	1.278(10)	C29−O5	1.317(11)
C6−O2	1.316(10)	C48−O8	1.317(11)	C6− O2	1.295(10)	C34−O6	1.286(10)
C1−C2	1.392(12)	C43−C44	1.384(13)	C1−C2	1.413(13)	C29−C30	1.423(13)
C2−C3	1.347(13)	C44−C45	1.425(14)	C2−C3	1.373(13)	C30−C31	1.336(13)
C3−C4	1.459(13)	C45−C46	1.401(13)	C3−C4	1.439(13)	C31−C32	1.426(13)
C4−C5	1.347(13)	C46−C47	1.325(13)	C4−C5	1.370(12)	C32−C33	1.362(12)
C5−C6	1.461(13)	C47−C48	1.428(13)	C5−C6	1.437(12)	C33−C34	1.408(13)
C1−C6	1.471(13)	C43−C48	1.459(13)	C1−C6	1.454(12)	C29−C34	1.431(13)
Catecholate Rings (Å)							
C15−O3	1.357(11)	C29−O5	1.329(11)	C15−O3	1.351(11)	C43−O7	1.330(11)
C20−O4	1.337(11)	C34−O6	1.356(10)	C20O4	1.358(10)	C48−O8	1.317(11)
C15−C16	1.399(14)	C29−C30	1.412(13)	C15−C16	1.379(12)	C43−C44	1.379(13)
C16−C17	1.386(13)	C30−C31	1.394(12)	C16−C17	1.369(12)	C44−C45	1.374(13)
C17−C18	1.396(14)	C31−C32	1.396(13)	C17−C18	1.406(21)	C45−C46	1.417(13)
C18−C19	1.383(14)	C32−C33	1.368(12)	C18−C19	1.367(12)	C46−C47	1.402(14)
C19−C20	1.395(13)	C33−C34	1.440(13)	C19−C20	1.377(12)	C47−C48	1.372(14)
C15−C20	1.392(13)	C29−C34	1.425(13)	C15−C20	1.437(12)	C43−C48	1.427(13)
Torsion Angles (deg)							
C64−C65−C67−C68		18.15		C64−C65−C77−C78		26.15	
C69−C70−C73−C74		30.03		C74−C75−C79−C78		35.33	
C64−C65−C73−C74		13.50		C64−C65−C75−C74		7.23	
Intermolecular Contacts (Å)							
O1(a)−C79(b)		3.192		C58(a)−C76(b)		3.340	
C58(a)−C80(b)		3.249		C76(a)−C58(b)		3.340	

increase approaching the upper temperature limit of our experiment, indicating that the values at 400 K are not likely to be limiting values and suggesting that switching to the $(Co^{II})_2$ form continues as the temperature is increased. Multiple sweeps from 2 to 400 K and back show no evidence of hysteresis. The data shown in Figure 4 were reproducible over several temperature sweeps.

X-ray Absorption Spectroscopy. Cobalt K-edge X-ray absorption (XAS) spectra were collected for **1** and **2** as polystyrene films, and the data are shown in Figure 5. The Co K-edges for both **1** and **2** are temperature dependent, and shift ca. 1 eV to higher energy when decreasing the temperature from 400 to 10 K. Similar behavior has been observed in the Co K-edge spectrum of a monomeric valence tautomer.[26] Interestingly, the shift in the Co K-edge is only half that observed in monomeric (N−N)Co(dioxolene)$_2$. Thus, for both **1** and **2**, between 10 and 400 K, only one of the two Co(dioxolene)$_2$ units undergoes valence tautomerism. The shift in the Co edge energy is consistent with an oxidation state change at the Co center. More specifically, an increase in the Co edge energy is consistent with a Co(II) → Co(III) conversion. As a means of standardization, we have measured the Co K-edge XAS spectrum of Pierpont's[25] Co^{III}(3,5-di-*tert*-butyl-SQ)(3,5-di-*tert*-butyl-Cat)(bipy) complex as a polystyrene film at 10 K (see Supporting Information) and found that there is no difference in energy compared to the spectra of compounds **1** and **2**. This indicates that at 10 K compounds **1** and **2** are in the $(Co^{III})_2$ form and therefore the shift observed as the temperature is decreased from 400 K is due to switching from the intermediate [(Co^{II})-(Co^{III})] form.

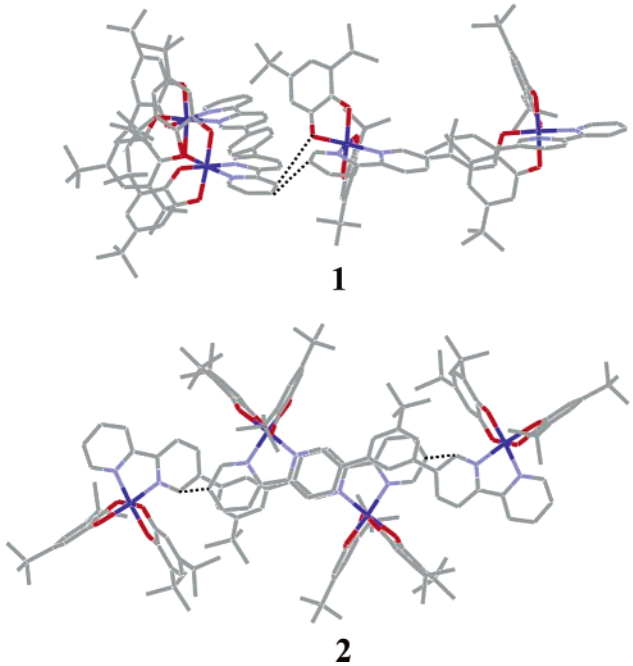

Figure 3. Intermolecular contacts less than 3.5 Å (···) between two molecules of complex **1** (top) and between two molecules of complex **2** (bottom) from the crystal structures. Hydrogen atoms and toluene molecules were omitted for clarity.

Electronic Absorption Spectroscopy. An intervalence charge transfer (IVCT) band (Figure 6), similar to that

(26) Roux, C.; Adams, D. M.; Itié, J. P.; Polian, A.; Hendrickson, D. N.; Verdaguer, M. *Inorg. Chem.* **1996**, *35*, 2846.

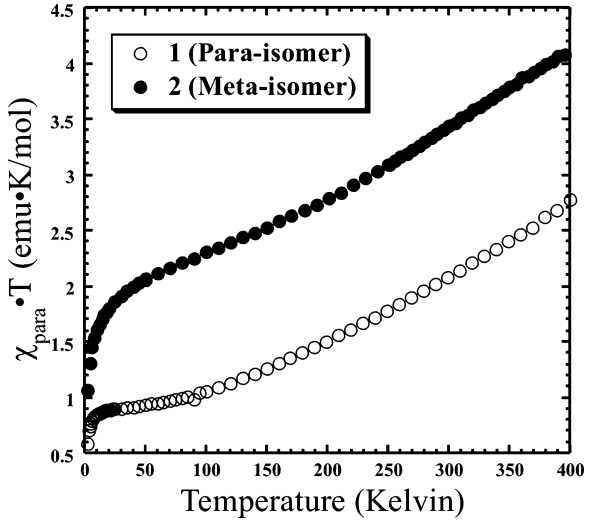

Figure 4. Temperature dependence of $\chi_{para}T$ for VT complexes **1** and **2**.

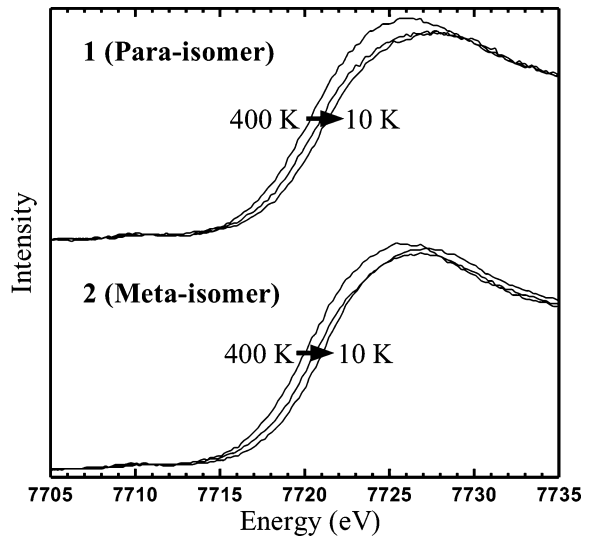

Figure 5. Temperature-dependent electronic absorption spectra for **1** and **2**.

observed in the monomeric Co−dioxolene complexes,[19] is present in the near-IR region of the electronic absorption spectra of **1** and **2**, measured as thin films prepared by evaporation of methylene chloride solutions under inert atmosphere. This IVCT band results from ligand mixed-valency in a single Co^{III} (SQ)(CAT) unit.[19] As such, this transition is a direct probe of electronic communication within a single VT unit, as well as between VT units. Furthermore, since an IVCT band is not expected for a Co^{II}-$(SQ)_2$ unit, the relative intensity of the absorption can be correlated directly to the concentration of Co^{III} in the sample. At the upper temperature limit where only the $(Co^{II})_2$ form is present, we expect an absorption of zero. At the lower temperature limit, where only the $(Co^{III})_2$ form is present, we expect the absorption intensity to plateau such that further lowering of temperature produces no change in the IVCT intensity. If there is strong interaction between the two cobalt centers, then we expect the change in intensity with temperature to decrease over some midpoint temperature range indicating partial isolation of the $[(Co^{II})(Co^{III})]$ form. The IVCT spectra were used to construct profiles of the mole

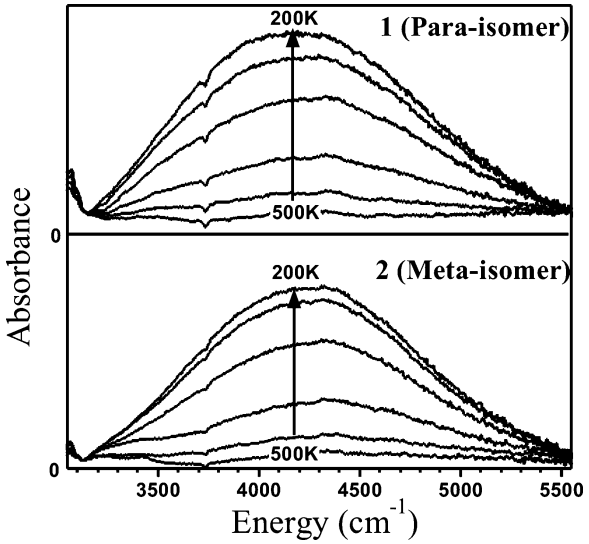

Figure 6. Temperature-dependent electronic absorption spectra (IVCT region) for **1** and **2** recorded between 500 and 160 K (**1**) and between 500 and 210 K (**2**). Optical densities below these temperatures remain constant.

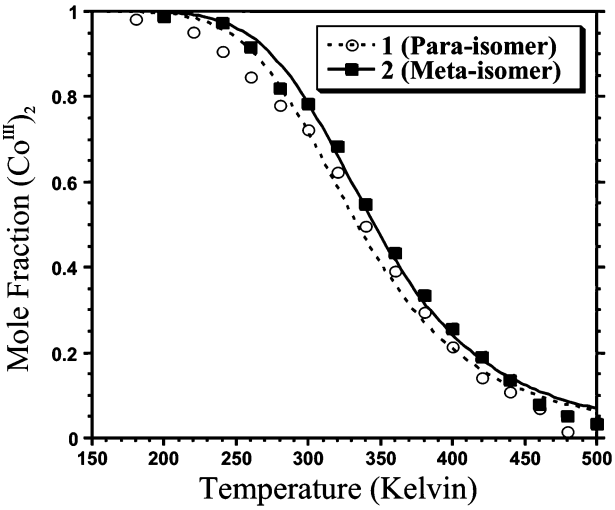

Figure 7. Temperature dependencies of IVCT band intensity for **1** and **2**.

fraction of the Co^{III} oxidation state using eq 1[27]

$$x_{Co(III)} = \frac{1}{\left[\exp\left(\frac{\Delta H^o}{RT} - \frac{\Delta S^o}{R}\right) + 1\right]} \qquad (1)$$

where $x_{Co(III)}$ is the mole fraction of Co^{III} per tautomer unit, and the other terms have their standard meanings. A value of $x_{Co(III)} = 0$ was assigned to the high-temperature plateau where no absorption was observed, as would be predicted for Co^{II} only. A value of $x_{Co(III)} = 1.0$ was assigned to the plateau at low temperature, where it is assumed that all the cobalt ions are in the Co^{III} oxidation state because of the fact that no further changes in peak intensity are observed at lower temperatures. The familiar sigmoidal shapes expected from a two-state equilibrium are obtained from the IVCT band intensities (Figure 7). Notably, the data for **1** and **2** are similar, showing conversion from the $(Co^{II})_2$ form

(27) Shultz, D. A.; Kumar, R. K.; Bin-Salamon, S.; Kirk, M. L. *Polyhedron* **2005**, *24*, 2876.

Table 2. Thermodynamic Parameters per Tautomeric Unit for **1** and **2** from IVCT Band Intensities

valence tautomer	$\Delta H°$ (kcal mol^{-1})	$\Delta S°$ (cal K^{-1} mol^{-1})
1 (para isomer)	-5.8 ± 0.3	-16.7 ± 0.7
2 (meta isomer)	-5.4 ± 0.4	-16.1 ± 1.0

(zero absorption intensity) over a 500 to 200 K temperature range, with no further change at lower temperature. The curve shows no inflection at the midpoint temperature of ca. 350 K. A least-squares fit was applied to the sigmoidal curves in Figure 7 to obtain thermodynamic parameters per tautomeric unit (Table 2) for the ls-Co^{III} to hs-Co^{II} conversions.

Discussion

The results of solid-state variable-temperature magnetic susceptibility studies on desolvated microcrystalline samples of **1** and **2** seem to reflect the differences in connectivity in these two species. In complex **1**, intramolecular coupling of the two Co centers may be mediated through the π system of the para-substituted central phenyl ring. Furthermore, intramolecular interactions through space may be facilitated by the proximity of the two Co centers. In complex **2**, the central phenyl ring is meta substituted giving rise both to different intramolecular interactions through the π system and to an inhibition of through-space intramolecular interactions. In keeping with this difference in connectivity, compound **1** switches from the [(Co^{II})(Co^{III})] form to the (Co^{III})$_2$ form at low temperature, whereas for complex **2** the magnetic data indicate that, in the same temperature range, conversion from the (Co^{II})$_2$ to the [(Co^{II})(Co^{III})] form is observed and further conversion to the isovalent (Co^{III})$_2$ form is incomplete even below 50 K, as seen in Figure 4.

These results do not correspond very well with those of the spectroscopic studies performed on samples of **1** and **2** as thin films or solid solutions as described above. Furthermore, the magnetometry results are in contradiction with the single-crystal X-ray structural data, collected on toluene-solvated crystalline material, which indicate that at ca. 125 K both **1** and **2** are in the (Co^{III})$_2$ form. Thus, these results underscore the importance of microscopic environment on VT equilibria. It has been shown that VT systems of this type are extremely sensitive to solvation,[28] and many of the apparent differences in switching temperature given by the various measurement techniques may be explicable as arising from differences in solvation.

The results of XAS measurements, performed on **1** and **2** as solid solutions (polystyrene films), indicate that both complexes exhibit the *same* behavior with regard to VT and exist, on average, in the [(Co^{II})(Co^{III})] form near 400 K and change to the (Co^{III})$_2$ form upon cooling to 10 K. Contrary to the magnetic susceptibility studies, but more consistent with XAS, electronic absorption spectroscopy (IVCT band) shows that thin films of **1** and **2** exhibit the *same* behavior (no difference between meta and para isomers); however, as measurements were performed over a wider temperature range, the data show that the (Co^{II})$_2$ form is accessible at high temperature.

We cannot definitively confirm that the (Co^{III})$_2$ form is accessed in the lower temperature limit of the IVCT band measurements; however, we speculate that this is the case given that there is no further increase in absorption intensity as the temperature is decreased below 200 K. We suggest that the IVCT band measurements do, in fact, access both the (Co^{II})$_2$ and the (Co^{III})$_2$ forms. It is more likely that the interaction between the two Co centers is negligible, such that there is a lack of inflection in Figure 7, than that the interaction is so strong that we can isolate the [(Co^{II})(Co^{III})] form and not switch to the (Co^{III})$_2$ form at low temperature. Thus, the experimental data for two noninteracting Co centers appear as they would for a single Co center. This is supported by the adequate fit of the data to eq 1. For both compounds, the IVCT band measurements indicate $\Delta H° \approx -5$ kcal/mol and $\Delta S° \approx -16$ eu as calculated per tautomeric unit. These values are within the range of previously studied mononuclear valence tautomers.[1] Since the absorbance of the IVCT bands tends toward zero at high temperature and levels off at low temperature, we propose that the (Co^{III})$_2$ and the (Co^{II})$_2$ electronic structures are realized, but that the intermediate form is not isolated due the fact that the two VT interconversions for both **1** and **2** are uncoupled. It may also be noted that the midpoint temperature of the IVCT band measurements (ca. 350 K) is close to the upper temperature limit of the XAS measurements (400 K) where the intermediate [(Co^{II})(Co^{III})] form exists, on average, in a polystyrene film.

Interestingly, both the electronic absorption measurements and the magnetometry measurements were preformed on desolvated samples, so the different outcomes cannot be attributed solely to differences in solvation. The difference in microscopic environment in this case is the difference between microcrystallinity and an amorphous film.

Conclusion

We have demonstrated that compounds **1** and **2** are the first complexes in which an ancillary diimine has been used as a bridging ligand to generate dinuclear VT compounds wherein all three possible valence tautomeric forms (Co^{III})$_2$, [(Co^{II})(Co^{III})], and (Co^{II})$_2$ are observed through a combination of magnetometry and spectroscopy in crystalline, solvated, and amorphous phases.

Combined studies of crystals and films using both magnetometry and spectroscopy are a good way to estimate relative contributions of intrinsic versus extrinsic effects on VT equilibria. Our conclusion is that para and meta isomers **1** and **2** display the same behavior in the absence of "crystal packing" and therefore, in this case, intermolecular interactions, not bipyridine electronic structure, make the largest contribution to $\Delta S°$. This result is not surprising considering the large number of bonds separating the metal ions. Therefore, if bipyridine ligand design is to be used as a design criterion for controlling VT, then more strongly coupled ligands are needed.[29]

Experimental Section

General. Starting materials were purchased and used without further purification unless otherwise stated. Elemental analyses were performed by Atlantic Microlab, Inc. High-resolution exact mass

(28) Hendrickson, D. N.; Pierpont, C. G. *Top. Curr. Chem.* **2004**, *234*, 63.

measurements were carried out by fast atom bombardment mass spectrometry (FAB-MS) with a JEOL (Tokyo, Japan) HX110HF mass spectrometer. The resolving power of the mass spectrometer was 10 000, the accelerating voltage 10 keV, and the ion source temperature 40 °C. NMR was performed at 200 MHz in *d*-chloroform, unless otherwise stated.

Synthesis of Complex 1. A Schlenk flask was charged with **5** (100 mg, 0.26 mmol) and purged with argon, then 15 mL of dry toluene was added, forming a solution. In a separate flask, cobalt semiquinone tetramer **9** (250 mg, 0.125 mmol) was dissolved in 10 mL of toluene. The solution of **5** was cannulated into the solution of **9,** and the reaction mixture was allowed to stir for 20 min and then sit under argon overnight. The solid green product was collected on a filter stick under argon. Yield: 58 mg (0.042 mmol based on two molecules of toluene per molecule **1** as indicated in the crystal structure, 16.8%).

Synthesis of Complex 2. A warm solution of **7** (58.6 mg, 0.132 mmol) in dry toluene (6 mL) under inert atmosphere was added dropwise to a warm solution of **9** (134.0 mg, 0.06706 mmol) in dry toluene (20 mL) under inert atmosphere. The resulting mixture was stirred at room temperature for 1.5 h. The solvent was removed in vacuo. The purple solid residue was recrystallized from toluene. Yield: 32.9 mg (0.0190 mmol based on three molecules of toluene per molecule **2** as shown in the crystal structure, 14.4%). Elemental analysis: C, 71.63% calcd, 71.69% found; H, 7.42% calcd, 7.53% found; N, 3.89% calcd, 3.18% found. FAB-MS: 1440.6675 *m*/*z*, 100%; 1441.6708 *m*/*z*, 99.0%; 1442.6740 *m*/*z*, 50.1%; 1443.68 *m*/*z*, 17.2%).

Synthesis of 1,4-Bis(4′-2′,2″-bipyridine)benzene (5). A degassed solution of $K_2CO_{3(aq)}$ (2 M, 1.6 mL), ethanol (1 mL), and THF was added to a flask containing 4-bromo-2,2′-bipyridine **3** (357 mg, 1.51 mmol), bisboronic ester **4** (200 mg, 0.606 mmol) and tetrakis(triphenylphosphine)palladium(0) (147 mg, 0.127 mmol) under inert atmosphere. The mixture was refluxed for 48 h. The solvent was removed in vacuo, and the residue was dissolved in methylene chloride (150 mL), washed with a saturated NaCl solution, and dried over Na_2SO_4. This solution was concentrated, MeOH (20 mL) was added, and the solution was cooled, resulting in the precipitation of a white powder from the brown solution. The precipitate was collected, washed with cold MeOH, and dried in vacuo. Yield: 180 mg (0.466 mmol, 76.9%). Physical properties were identical to those previously reported.

Synthesis of 1,3-Bis(4′-2′,2″-bipyridine)-5-*t*-butylbenzene (7). Ethanol (0.5 mL) was added to a Schlenk flask containing 4-bromo-2,2′-bipyridine **3** (198.6 mg, 0.8448 mmol), bisboronic ester **6** (128.5 mg, 0.3328 mmol) and tetrakis(triphenylphosphine)palladium-(0) (82.7 mg, 0.076 mmol). The flask was degassed, and an inert atmosphere was introduced. Aqueous (2 M) Na_2CO_3 (0.8 mL) was added followed immediately by 10 mL of dry THF. The flask was degassed and then refluxed under inert atmosphere for 18 h. Once cooled to room temperature, the solvent was removed in vacuo yielding a pale solid and a yellow liquid. This residue was dissolved in methylene chloride, filtered through a plug of Celite, washed with a saturated aqueous solution of ammonium chloride, and dried over magnesium sulfate. The solvent was removed in vacuo. The solid white product was separated from the residue by chromatography (alumina stationary phase, 1:1 CH_2Cl_2/petroleum ether moving phase, then flushed with CH_2Cl_2). Yield: 68.9 mg (0.156 mmol, 46.9%). ^{1}H NMR ($CDCl_3$): 8.99 (d, 2H, 1.2 Hz), 8.72 (d, 2H, 2.6 Hz), 8.53 (d, 2H, 5.5 Hz), 8.48 (d, 2H, 5.3 Hz), 8.10 (dd, 2H, 5.5 Hz, 1.6 Hz), 7.86 (dt, 2H, 1.1 Hz, 5.2 Hz), 7.72 (s, 2H + 1H), 7.35 (dt, 2H, 1.0 Hz, 4.3 Hz), 1.47 (s, 9H).

Magnetometry. Magnetic susceptibilities were measured on a Quantum Design MPMS-XL7 SQUID magnetometer using an applied field of 1 T for Curie plots. Data were corrected for molecular diamagnetism using Pascal's constants. Microcrystalline samples were loaded into the sample space of a Delrin sample holder and mounted directly to the sample rod. The sample holder measurement was subtracted out using an empty Delrin sample holder as the background.

X-ray Crystallography. Details for **1** and **2** are listed in Supporting Information.

Electronic Absorption Spectroscopy. Electronic absorption spectra were collected in the mid- to near-IR region. Experiments were performed on a Digilab FTS 3000 FTIR spectrometer equipped with a globar source, KBr beam splitter and a liquid nitrogen cooled MCT detector. Thin films were prepared by evaporation of CH_2Cl_2 solutions onto ZnSe plates under inert atmosphere. The reported spectra are the average of 64 scans at a spectral resolution of 2 cm^{-1}. The temperature-dependent spectra were recorded using a helium cooled cryostat (MicrostatHe, Oxford Instruments).

X-ray Absorption Spectroscopy. Cobalt XAS spectroscopy was performed at SSRL beamline VII-3, under dedicated conditions (3.0 GeV, 100 mA), using a Si(220) double-crystal monochromator detuned to 50% of the maximum intensity to eliminate harmonics. X-ray energies were calibrated by simultaneous measurements of the absorption spectrum of a Co foil, with the first inflection point assigned as 7709 eV. Spectra were measured using 10 eV steps in the preedge region, 0.2 eV in the edge region, and 0.1 eV in the postedge region with integration times of 1, 2, and 1 s, respectively for a total scan time of ca. 20 min. Data were collected as fluorescence excitation spectra using a 30-element Ge solid-state detector array. Each channel of each scan was individually evaluated for quality and then averaged (16 per scan) to yield the final spectra. Care was taken to avoid detector saturation. Samples were prepared as polystyrene thin films for cobalt dimer and monomer samples. Cobalt standards, $Co(acac)_3$ and $CoCl_2$, were run as solid samples in boron nitride. Temperature control for scans at or below 150 K was achieved with a helium flow cryostat. Temperatures at or above room temperature were maintained using a custom-designed spectroscopic furnace heated by a reversed Peltier-diode. The aluminum furnace sample chamber was built to be compatible with a Hitachi U-3501 spectrophotometer as well as the synchrotron beamline. Hence, the sample chamber has two possible configurations: absorbance mode, with the sample orthogonal to the incident photons, and fluorescence mode, with the sample oriented 45° degrees to the incident photons. Helium gas was used to purge the sample space to prevent air from contacting and contaminating the sample.

Acknowledgment. D.A.S. thanks the National Science Foundation for funding (Grant CHE-0345263; SQUID magnetometer, Grant CHE-0091247), as well as the Camille and Henry Dreyfus Foundation for a Camille Dreyfus Teacher-Scholar Award. K.E.P. thanks NSERC for PDF funding.

Supporting Information Available: X-ray crystallographic files for **1** and **2** in CIF format and relevant crystallographic data; graph showing XAS comparison of **1** and **2** to a known compound at 10 K. This material is available free of charge via the Internet at http://pubs.acs.org.

IC060170Y

(29) Balzani, V.; Barigelletti, F.; Belser, P.; Bernhard, S.; De Cola, L.; Flamigni, L. *J. Phys. Chem.* **1996**, *100*, 16786.